Modeling Electromagnetic Propagation in the Earth–Ionosphere Waveguide

Steven A. Cummer, *Member, IEEE*

***Abstract*—The ionosphere plays a role in radio propagation that varies strongly with frequency. At extremely low frequency (ELF: 3–3000 Hz) and very low frequency (VLF: 3–30 kHz), the ground and the ionosphere are good electrical conductors and form a spherical earth–ionosphere waveguide. Many giants of the electromagnetics (EMs) community studied ELF-VLF propagation in the earth–ionosphere waveguide, a topic which was critically important for long-range communication and navigation systems. James R. Wait was undoubtedly the most prolific publisher in this field, starting in the 1950s and continuing well into the 1990s. Although it is an old problem, there are new scientific and practical applications that rely on accurate modeling of ELF-VLF propagation, including ionospheric remote sensing, lightning remote sensing, global climate monitoring, and even earthquake precursor detection. The theory of ELF-VLF propagation in the earth-ionosphere waveguide is mature, but there remain many ways of actually performing propagation calculations. Most techniques are based on waveguide mode theory with either numerical or approximate analytical formulations, but direct finite-difference time-domain (FDTD) modeling is now also feasible. Furthermore, in either mode theory or FDTD, the ionospheric upper boundary can be treated with varying degrees of approximation. While these approximations are understood in a qualitative sense, it is difficult to assess in advance their applicability to a given propagation problem. With a series of mode theory and FDTD simulations of propagation from lightning radiation in the earth–ionosphere waveguide, we investigate the accuracy of these approximations. We also show that fields from post-discharge ionospheric currents and from evanescent modes become important at lower ELF ($\lesssim 500$ Hz) over short distances ($\lesssim 500$ km). These fields are not easily modeled with mode theory, but are inherent in the FDTD formulation of the problem. In this way, the FDTD solution bridges the gap between analytical solutions for fields close to and far from the source.**

***Index Terms*—Earth–ionosphere waveguide.**

I. Introduction

THE ionosphere, the electrically conducting region of the upper atmosphere, plays a role in essentially all radio propagation. That role can be small, as for gigahertz signals, which acquire an uncertain group delay [1, p. 251] and scintillation-induced incoherence [2] from the ionosphere. For lower frequencies, however, the ionosphere is more than just a perturbation and strongly reflects high-frequency (HF) and lower frequency waves [3]. Even Marconi's original transatlantic radio transmission was assisted by the ionosphere, as was realized when calculations showed that purely ground-guided propagation could not account for the observed field strengths [4]. This confirmed the existence of a spherical shell waveguide formed by the ground and the conducting ionosphere, which is commonly referred to as the earth–ionosphere waveguide.

At extremely low frequency (ELF: 3–3000 Hz) and very low frequency (VLF: 3–30 kHz), the ionosphere strongly affects propagation even over short paths. ELF-VLF wave propagation in the earth–ionosphere waveguide was a problem to which many of the giants of the electromagnetics (EMs) community contributed, including Wait, Budden (both of whom have won the IEEE Hertz Medal), and Booker. At the time of their main contributions, understanding and predicting long-wave propagation was critically important for long range communication and navigation systems. However, these researchers were probably attracted to the problem as much for its theoretical challenge as for its practical applications.

James R. Wait was undoubtedly the most prolific publisher in this field. He solved many fundamental propagation problems analytically (e.g., [5]), and analyzed many realistic propagation problems that were best treated numerically (e.g., [6]). He also produced fundamental formulations for scattering from localized inhomogeneities in the earth–ionosphere waveguide [7]. Wait's work in this area continued even in recent years in the analysis of propagation in the presence of large-scale [8] and small-scale [9] inhomogeneities in the waveguide.

Although it is an old problem, and the original applications of navigation and long distance communication are no longer as relevant, thanks to global positioning systems (GPSs) and satellite communication (though submarine communication still relies on VLF transmitters), there are new scientific and practical applications that rely on accurate modeling of ELF-VLF propagation. The sensitivity of ELF-VLF propagation to the lower ionosphere makes it an ideal probe for remotely sensing the ambient state [10] and localized perturbations [11], [12] of the ionosphere. Lightning is by far the strongest natural source of ELF-VLF waves on the ground and the combination of observations and modeling form a powerful technique for detecting and pinpointing discharges [13] and for remotely measuring lightning currents [14], [15]. This latter technique has been applied with great success to quantifying the discharges which produce sprites [16], the recently discovered high-altitude optical emissions associated with big lightning discharges [17]. Global lightning rates measured from subionospheric ELF observations may be a sensitive monitor of global temperature change [18]. ELF-VLF waves have long been used for subsurface remote sensing and geophysical prospecting [19] and subionospheric VLF wave propagation irregularities [20] and unusual ELF-VLF wave generation [21] have even been impli-

Manuscript received September 6, 1999; revised March 6, 2000.

The author is with the Electrical and Computer Engineering Department, Duke University, Durham, NC 27708 USA (e-mail: cummer@ee.duke.edu).

Publisher Item Identifier S 0018-926X(00)09371-6.

cated as precursors to major earthquakes, although this assertion remains rather controversial.

While the theory of ELF-VLF propagation in the earth–ionosphere waveguide is mature, there remain many ways of implementing propagation calculations. Most techniques are based on waveguide mode theory [22], with either numerical or approximate analytical formulations, but direct finite-difference time-domain (FDTD) modeling is now also feasible. Finite-element methods have also been used [23]. Furthermore, in any of these techniques, the ionospheric upper boundary can be treated with varying degrees of approximation. While these approximations are understood in a qualitative sense, it is difficult to assess their applicability to a given propagation problem. With a series of mode theory and FDTD solutions to the earth–ionosphere waveguide propagation problem, we investigate the accuracy of these approximations and discuss the relative advantages of mode theory and FDTD techniques. As our benchmark problem, we consider the broad-band propagation of an ELF-VLF signal radiated by a lightning discharge. This problem is more closely related to the modern applications mentioned above than is the canonical problem of calculating the field strength as a function of distance from a single frequency transmitter. The broad-band problem also highlights some important effects not produced in single frequency propagation. Historically, the single mode regime below 1.6 kHz has been treated separately from the multimode VLF regime above this frequency, no doubt due to the easier analytical treatment of single mode propagation. However, they are essentially the same problem and we treat them together in this work.

In general, we find excellent agreement between mode theory and FDTD calculations. The validity of the various approximations considered varies significantly and depends somewhat on the ambient state (daytime or nighttime) of the ionosphere. We also find that mode theory gives good results at VLF at distances as short as 100 km from the source, but for frequencies less than ~ 2 kHz, the difference between mode theory and FDTD grows as frequency and distance decrease. We attribute this difference to two factors. First, evanescent modes excited by the discharge contribute to the fields when the propagation distance is short. With care, however, these fields can be accounted for in mode theory. Second, the zero frequency component of the lightning source (i.e., the net charge motion) creates secondary, postdischarge currents in the ionosphere, which generate their own fields. These post-discharge fields are not accounted for in traditional mode theory but are implicitly generated in the FDTD solution. This emphasizes a strength of the FDTD solution in that it inherently combines the fields produced by the discharge and post-discharge sources, which are generally treated separately in the literature. These post-discharge fields can be significant for $f \lesssim 500$ Hz over short propagation paths and may need to be accounted for in interpreting ELF lightning observations.

II. Problem Formulation

Fig. 1 shows the physical configuration of the problem. A vertical electric dipole source, either transient or time harmonic, radiates on the ground in the free-space region of altitude extent

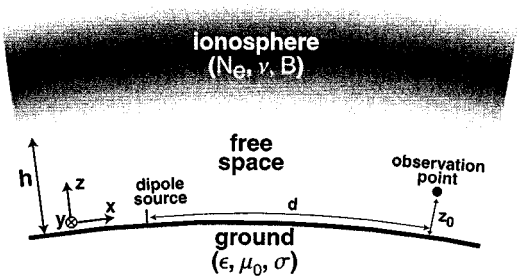

Fig. 1. Geometry and coordinates of the earth–ionosphere waveguide propagation problem.

h between the ionosphere and ground. We wish to calculate the electric and magnetic fields at some remote location at a horizontal distance d from the source and at altitude z_0. While the problem geometry is spherical, it can be treated as Cartesian for propagation paths significantly shorter than the radius of the earth. We assume such an approximation in this work for the sake of simplicity, although Wait [24] and Galejs [25] have derived formulations for cylindrical and spherical waveguides as well as for horizontally aligned sources.

A. Waveguide Boundaries

The ground is assumed homogeneous with permeability μ_0, conductivity σ_g, and relative permittivity ϵ_r. This treatment is valid as long as the medium is vertically homogeneous over a few skin depths (generally a few kilometers at this frequency range), which is true over ocean and most land but not over the low-conductivity polar ice caps. The ionosphere is most generally treated as an inhomogeneous and anisotropic cold plasma, which is valid as long as the wave power is not so high that the medium is modified by the wave itself. Lightning radiation can be strong enough to violate this assumption [26], but this only occurs near the source and does not play a significant role in the long-distance propagation studied here.

The EM fields in a cold plasma are described by Maxwell's equations coupled to equations for current derived from the Lorentz equation of motion of the charged particles in the medium in response to the wave electric field and an ambient static magnetic field from the earth [27, p. 45]

$$\partial \boldsymbol{J}_n/\partial t + \nu_n \boldsymbol{J}_n = \frac{q_n}{|q_n|}\,\omega_{Bn}(\boldsymbol{J}_n \times \boldsymbol{b}_E) + \epsilon_0 \omega_{pn}^2 \boldsymbol{E} \quad (1)$$

where ω_{pn} is the plasma frequency of each type of particle, ω_{Bn} is the gyrofrequency of each and ν_n is the momentum transfer collision frequency of each. The vector $\boldsymbol{b}_E$ is defined as the unit vector in the direction of the static magnetic field of the earth $\boldsymbol{B}_E$. Each important charged species makes its own contribution to the total current, which is defined as $\boldsymbol{J}_{tot} = \sum_n \boldsymbol{J}_n$. The total current is then folded back into Maxwell's equations, thereby completing the system.

Fig. 2 shows typical altitude distributions of free electron and positive ion number densities (although they are actually "concentrations," the historically correct term is density) in the ionosphere for both day and night and typical collision frequencies as a function of altitude (which do not depend on local time).

Negative ions are also present in the number density required by charge neutrality. Solar radiation is the source of most of the free electrons during daytime, while nonsolar ionizing sources such as precipitating energetic electrons, meteoric ionization, and cosmic rays, maintain the free electron concentration at night [28, p. 231]. The difference between day and night affects the validity of certain approximations for ELF–VLF wave propagation, as is discussed below. The contribution of the ions to the total current is often neglected in earth–ionosphere waveguide calculations, but their effect is significant, particularly at ELF where their higher number density at low altitudes makes them the dominant contributor to the conductivity of the ionosphere.

B. Mode Theory

Maxwell's equations and (1) can be solved directly by finite-difference techniques (and they will be below), but the method that is most amenable to analytical treatment, that provides physical insight, and that was used by Wait, Budden, and others in their original formulations, is mode theory. Mode theory is inherently a time harmonic formulation (we assume an $e^{i\omega t}$ variation), but wide-band time-domain problems can be solved through analytical or numerical Fourier transforms. Although Wait and Budden pursued their research independently, they arrived at essentially equivalent formulations of this problem. Wait's formulations were published over the course of many papers in the 1950s and 1960s and are very conveniently assembled in his classic book [24]. This formulation is summarized below. Budden's formulation [29] is the basis of the numerical mode theory model developed by the U.S. Navy [30] that we use for the modal calculations in this work.

As in Fig. 1, consider a vertical electric current source of current moment M_I (current times channel length) in free-space, radiating at a single-frequency ω located at the origin and oriented in the z direction. The waveguide is a completely general free-space-filled two-dimensional (2-D) waveguide—a slab of free-space sandwiched between two reflecting layers. These reflecting layers can be composed of any material that produces some reflection back into the free-space region from outward propagating waves. This important abstraction makes this formulation applicable to essentially any 2-D waveguide regardless of size and of bounding material.

In the free-space region, symmetry implies that the fields can be separated into the usual TE and TM groups, which can be treated independently in an isotropic waveguide. However, since the ionosphere is a magnetized plasma and thus is anisotropic, these field groups are coupled at the upper boundary and an incident TE or TM wave produces both TE and TM reflections. Purely TE or TM propagation thus is not possible in the earth–ionosphere waveguide. The coupling between the fields means that the reflection coefficient from the upper boundary is not a scalar but is rather a 2×2 matrix, where each matrix element is one of the four different reflection coefficients for a specific incident and reflected polarization. The lower boundary of the earth–ionosphere waveguide is the ground, which is isotropic so that the cross-polarized reflection coefficients in the ground reflection matrix are zero.

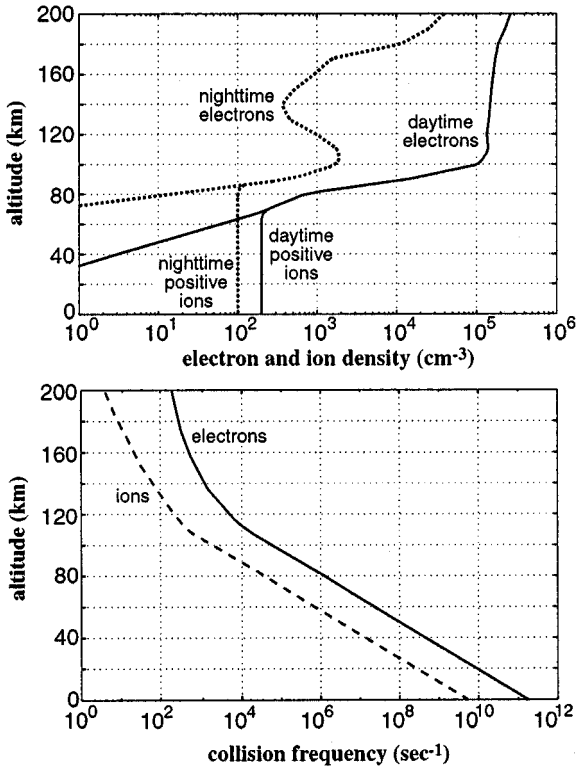

Fig. 2. Representative daytime and nighttime ionospheric electron and ion number density profiles and collision frequency profiles.

We define $\boldsymbol{R}_I$, the reflection matrix of the ionosphere at altitude $z = h$, and $\boldsymbol{R}_G$, the reflection matrix of the ground at $z = 0$, as

$$\boldsymbol{R}_I(\theta) = \begin{bmatrix} {}_{\parallel}R^i_{\parallel} & {}_{\parallel}R^i_{\perp} \\ {}_{\perp}R^i_{\parallel} & {}_{\perp}R^i_{\perp} \end{bmatrix} \quad \boldsymbol{R}_G(\theta) = \begin{bmatrix} {}_{\parallel}R^g_{\parallel} & 0 \\ 0 & {}_{\perp}R^g_{\perp} \end{bmatrix}. \quad (2)$$

These reflection coefficients are implicitly functions of the angle of incidence. The left subscript on the matrix elements denotes the incident wave polarization (parallel or perpendicular to the plane of incidence containing the wave vector and the boundary normal) and the right subscript denotes the reflected polarization.

By using the plane wave spectrum representation of the fields from a source dipole, postulating a particular solution form in the presence of the waveguide and enforcing continuity of the tangential field components, Wait shows that the fields in the waveguide, in terms of the electric and magnetic Hertz vectors $\boldsymbol{U}$ and $\boldsymbol{V}$ (from which electric and magnetic field components are easily recovered [31, p. 29]) are given by [24, p. 248]

$$\begin{bmatrix} U_z \\ V_z \end{bmatrix} = -\frac{kM_I}{8\pi\omega\epsilon_0} \int_\Gamma \boldsymbol{F}(C) \begin{bmatrix} 1 \\ 0 \end{bmatrix} H_0^{(2)}(kSx)\, dC \quad (3)$$

with

$$\boldsymbol{F}(C) = \frac{(e^{ikCz} + \boldsymbol{R}_G(C)e^{-ikCz})(e^{ikCh} + \boldsymbol{R}_I(C)e^{-ikCh})}{e^{ikCh}(1 - \boldsymbol{R}_G(C)\boldsymbol{R}_I(C)e^{-2ikCh})} \quad (4)$$

where C and S are the cosine and sine of the complex angle of incidence θ of the wave on the upper and lower boundaries. $H_0^{(2)}(x)$ is the Hankel function of zero order

and second kind. The integrand contains poles where $\det(1 - \boldsymbol{R}_G(C)\boldsymbol{R}_I(C)e^{-2ikCh}) = 0$ and, thus, the integral can be evaluated as a residue series. This pole equation is commonly referred to as the mode condition and it requires that one eigenvalue of the net reflection coefficient $\boldsymbol{R}_G\boldsymbol{R}_I e^{-2ikCh}$ be unity. This is equivalent to stating that the plane wave at the given incidence angle reflected once each from the upper and lower boundaries must be in phase with and equal in amplitude to the incident plane wave [32, p. 691]. Each angle of incidence θ_n that satisfies the mode condition is referred to as an eigenangle and defines a waveguide mode at the frequency ω under consideration. The index of refraction of a mode is simply $\sin\theta$, thus, the eigenangle contains all the necessary information about the phase velocity and attenuation rate. Because the boundaries are lossy in the earth–ionosphere waveguide (due to both absorption in the boundaries and wave leakage), the eigenangles are necessarily complex. In this way, the fields in the waveguide can be thought of as the sum of contributions from the angular spectrum of plane waves at angles for which propagation in the waveguide is self-reinforcing. Budden [22], rather than postulating a solution form and solving the boundary value problem, arrived at an essentially identical formulation by summing the fields produced by an infinite number of sources, each corresponding to a different multiply reflected plane wave in the waveguide.

The fields are thus given by the residue series

$$\begin{bmatrix} U_z \\ V_z \end{bmatrix} = \frac{ikM_I}{4\omega\epsilon_0} \sum_n \frac{e^{2ikC_n h}}{\partial\Delta/\partial C|_{\theta=\theta_n}} \begin{bmatrix} \left(e^{2ikC_n h} - {}_{\perp}R^g_{\perp\perp}R^i_{\perp}\right) f^1_p(z) \\ i_{||}R^g_{||||}R^i_{\perp} f^2_p(z) \end{bmatrix} H^2_0(kS_n x) \quad (5)$$

where $\Delta(C) = \det(e^{2ikCh} - \boldsymbol{R}_G\boldsymbol{R}_I)$. Each term in (5) has a physical interpretation. The leading constant is a source term which depends on the current-moment M_I of the vertical dipole source. The first term in the summation is commonly referred to as the excitation function for a particular mode at a given frequency and it quantifies the efficiency with which that mode is excited by a vertical dipole on the ground. The 2×1 matrix in the summation describes the field variation with altitude and the functions f^1_p and f^2_p are defined explicitly in [24, p. 249]. The $H^2_0(kS_n x)$ term describes the propagation of a cylindrically expanding wave, which exists because the expansion in the vertical direction is limited by the waveguide boundaries so that the mode fields spread only horizontally. The summation is over an infinite number of modes, but in practice it can be limited only to the modes which contribute significantly to the fields at a distance d from the source. Often for long distances, only a few low attenuation modes contribute significantly to the fields, leading to a very compact and efficient calculation. For very short distances, however, even evanescent or highly attenuated modes can contribute to the fields [33] and mode theory becomes less efficient and more difficult to implement. Conveniently, with FDTD, short propagation paths are significantly easier to model than long paths because of the smaller simulation space required.

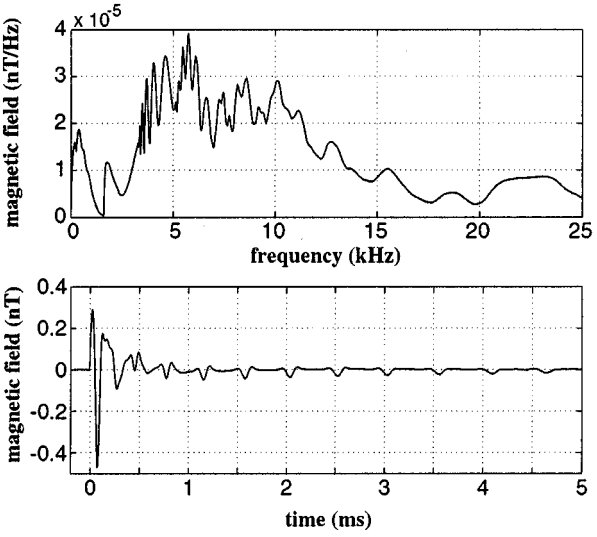

Fig. 3. Sample mode theory calculation for a transient source 1000 km from the receiver. (a) Magnetic field amplitude as a function of frequency. (b) Magnetic field waveform as a function of time, calculated with a numerical inverse Fourier transform.

C. Sample Mode Theory Calculation and Observations

If the reflection coefficients for the upper and lower waveguide boundaries can be calculated analytically, then the radiated fields can also be found analytically through (5). This can be done for simple treatments of the ionospheric upper boundary, like a sharp dielectric boundary or wave impedance condition, and many of these solutions can be found in [24] and [25]. However, the reflection coefficient of a realistic ionosphere must be calculated numerically. A complete 2-D waveguide propagation formulation was implemented in a series of programs called long wave propagation code (LWPC) that was developed over many years at the Naval Ocean Systems Center [30]. We use these programs for our mode theory calculations throughout this work.

As a sample calculation, we consider the signal received at a distance of 1000 km, which is radiated by a lightning discharge (a broad-band source) whose current is given by

$$I(t) = 3.74 \times 10^4 \left(e^{10^4 t} - e^{5\times 10^4 t}\right) A \quad (6)$$

with t in seconds. This gives a peak current of 20 kA and the lightning channel length is assumed to be 1 km. This discharge is a close approximation to the typical discharge described in [34]. The signal is propagated between the nighttime ionosphere of Fig. 2 and a ground of $\epsilon_{rg} = 15$ and $\sigma_g = 10^{-2}$ S/m. We use an ambient magnetic field typical of that over the United States, which contains significant vertical and horizontal components. Fig. 3(a) shows the amplitude of the horizontal TM field (B_y in the coordinate system of Fig. 1) as a function of frequency calculated with the LWPC mode theory code. Despite the apparent complexity, the signal is similar to what would be observed in a perfectly conducting parallel-plate waveguide. Between 0 and ~1600 Hz, there is a single propagating mode that is analogous to the parallel-plate waveguide transverse EM (TEM) mode (although the anisotropy of the upper boundary means that the mode is only quasi-TEM). At ~1600 Hz, the amplitude

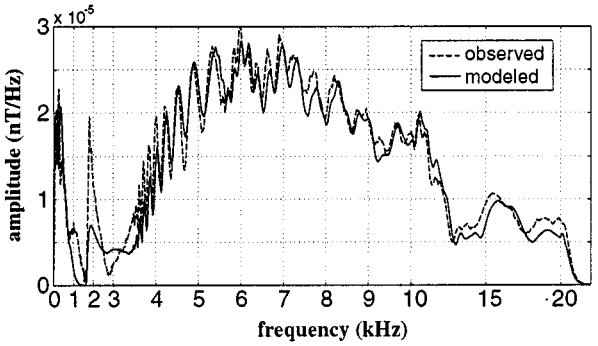

Fig. 4. Comparison of observed and modeled ELF-VLF spectra. Note the nonlinearity of the horizontal scale. The good agreement shows that mode theory accurately models reality if the proper ionosphere is used in the calculations. Adapted from [10].

rises sharply when the cutoff frequency of the first dispersive mode is crossed and the signal from the equivalent of the TE_1 and TM_1 modes contributes to the signal (in reality, only the quasi-TE_1 mode contributes as the quasi-TM_1 mode attenuation is very high). As the frequency increases, additional modes appear as integer multiples of the cutoff frequency are crossed, again just as in a parallel-plate waveguide. The mutual interference of these modes changes strongly with frequency, which accounts for the complicated variation of amplitude at frequencies where many modes contribute to the signal. The apparent cutoff frequency of about 1.6 kHz gives an effective waveguide height of about 94 km. Approximately 15 modes contribute significantly to the signal at 20 kHz and this number increases with increasing frequency.

The complex spectrum resulting from the mode theory calculation can easily be converted to a time-domain waveform through the Fourier transform, which we approximate using the fast Fourier transform (FFT). Fig. 3(b) shows the magnetic field waveform corresponding to the complex spectrum in Fig. 3(a). Most of the transient signal's energy arrives in the early portion of the waveform, but there is a strongly dispersed component near the cutoff frequencies, where the group velocity becomes significantly lower than the speed of light, again just as in a parallel-plate waveguide. This tail can be also interpreted as a series of multiple reflections from the waveguide walls [22].

Since this model uses an arbitrary (and therefore realistic) ionosphere as the basis for its calculations, it can represent reality quite closely (as shown in Fig. 4) by the comparison between measurements and mode theory (adapted from [10]). Fig. 4 shows the ELF–VLF spectrum measured from the radiation from multiple lightning discharges and the spectrum calculated from mode theory along the same propagation path. If the proper realistic ionosphere is used in the mode theory calculations, then theory can be made to match experiment very closely.

D. Mode Theory and Post-Discharge Fields

For single-frequency radiation problems, mode theory is an essentially exact formulation. However, for the lightning discharge problem (or any other problem with zero frequency excitation), mode theory does not explicitly include all of the EM fields. Not only is an electrostatic field created by the lightning charge transfer between cloud and ground, but the ionospheric conductivity variation with altitude means that slowly varying post-discharge currents are generated in the ionosphere, which create their own EM fields. These post-discharge currents and fields are not accounted for in traditional mode theory and can be significant at lower ELF frequencies over short ($\lesssim$500 km) propagation paths. Greifinger and Greifinger [35] published an extremely insightful analysis of these postdischarge currents and fields, which were analyzed numerically in [36]. Sukhorukov [33] derived an approximate analytical solution for the lightning-induced fields which includes both the discharge (i.e., mode theory) and post-discharge ionospheric relaxation fields. The FDTD solutions presented here also inherently combine these two sources and the differences between mode theory and full wave FDTD with respect to these post-discharge fields are discussed in detail in Section V-D.

III. Mode Theory Approximations

While the ionosphere is most generally treated as an anisotropic cold plasma, there are approximations which can simplify and accelerate the calculations and still provide useful results. One class of approximations are simplifications to the anisotropic cold plasma medium. If $\nu \gg \omega$ for all frequencies of interest and at all altitudes where the wave is expected to penetrate significantly, then the $\partial \boldsymbol{J}/\partial t$ term in (1) can be neglected relative to the $\nu \boldsymbol{J}$ term. This approximation yields a medium in which $\boldsymbol{J}$ is a linear function of $\boldsymbol{E}$ and is thus an anisotropic but frequency-independent conductor rather than a plasma. We call this the anisotropic conductor approximation. Similarly, if $\nu \gg \omega_B$ at all important altitudes, then the cross terms in (1) are negligible and the medium becomes an isotropic plasma. If these approximations are both valid, then the ionosphere can be treated as an isotropic conductor with conductivity $\sigma_i = \epsilon_0 \omega_p^2/\nu$. These assumptions are commonly invoked in problems of daytime earth–ionosphere waveguide propagation because the enhanced electron density relative to night limits the wave penetration to lower altitudes.

The second class of approximations are fully analytic solutions, which assume simplified electron density profiles and magnetic field orientation and restrict the frequency range. Greifinger and Greifinger [37] solved single-mode ELF propagation assuming exponentially increasing ionospheric conductivity and including the effect of a vertical ambient magnetic field. An earlier approximation [38], which neglects the magnetic field entirely is really only applicable to highly disturbed daytime ionospheres and we do not include it in our analysis. Wait [39] presented an alternate derivation of these formulations that includes an extension to nonperfectly conducting ground. Sukhorukov [40] formulated an analytical approximation to the propagation near the cutoff frequency of the first few modes, which form the dispersed tail (sometimes referred to as a "tweek" [41] because of its sound when played on a loudspeaker) of the transient waveform radiated by lightning. When not neglected entirely, the magnetic field is assumed vertical in these formulations for simplicity.

IV. FDTD

Pure propagation problems with complicated inhomogeneities, like those considered here, can be very easily solved with FDTD techniques. Because the source is vertically aligned, we can treat the problem as 2-D in cylindrical coordinates with azimuthal symmetry. The ground is assumed a perfect conductor, and the ionosphere is vertically inhomogeneous but treated with the anisotropic conductor approximation described above. The ambient magnetic field is vertically oriented to simplify the problem, though we show below that this can be a restrictive assumption. The noncollocation of field components in the standard leapfrog FDTD formulation means that the cross terms in the electric field iterations (i.e., E_r in the update for E_z, etc.) that result from the ionospheric anisotropy must be spatially averaged to ensure second-order accuracy. Absorbing boundary conditions can be simply implemented even for the anisotropic and dispersive medium in cylindrical coordinates with the stretched field formulation for the perfectly matched layer (PML) [42]. This yields an apparently stable simulation, though this assertion is based only on numerical experimentation rather than rigorous analysis.

For the FDTD simulations in this work, we use a spatial step size of 1 km in z and r and a time step at the Courant limit for a two dimensional simulation. The PML thicknesses are 40 and 80 cells on the z and r boundaries. These unusually thick PML layers are required to absorb sufficiently the long wavelength ELF frequencies. We impose a transient vertical current source at the origin with current given by (6) and thereby solve the precisely same problem as we did with mode theory.

The FDTD technique has certain advantages over mode theory. FDTD directly calculates the fields in the ionosphere, which is difficult in mode theory. Though modeled here, complicated horizontal inhomogeneities can be easily included in an FDTD simulation, while mode theory requires complicated mode conversion calculations in the presence of such inhomogeneities [30]. However, mode theory still retains a significant speed advantage in many problems compared to FDTD. Specifically, once the complete set of modes for a given problem is found, the fields at any free-space altitude and any distance from the source can be very rapidly calculated from a mode sum like (5). With FDTD, there is always a computer memory imposed limit to the size of the problem that can be solved, although this limit is continually increasing.

V. Solution Comparisons

While the utility of the mode theory approximations mentioned above, especially the fully analytical ones, cannot be denied, it is not always clear under what conditions they are or are not valid. We use the same transient source and propagation over a 1000-km path to investigate the accuracy of the various modeling techniques described above, using mode theory with a fully anisotropic cold plasma ionosphere as the benchmark solution. As mentioned above, we use an ambient magnetic field typical of that over the United States, which contains significant vertical and horizontal components. The ionosphere is always assumed horizontally homogeneous, but we consider separately nighttime and daytime ionospheres as the effect of the approximations differ in each case.

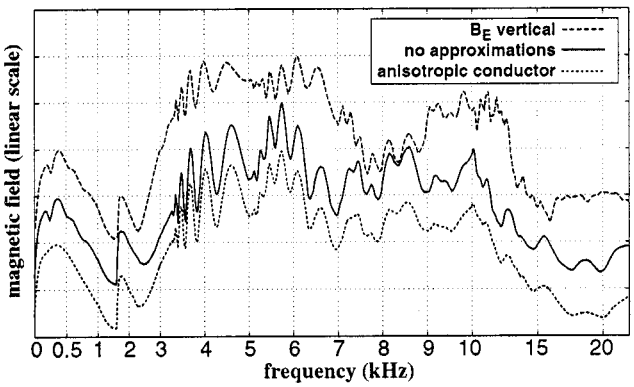

Fig. 5. Nighttime ELF-VLF spectra computed with mode theory for different ionospheric approximations. Note the nonlinearity of the horizontal scale. The curves are offset by one grid unit each.

A. Nighttime Ionosphere

Fig. 5 shows horizontal magnetic field amplitude spectra for transient 1000 km propagation calculated with the LWPC mode theory model with a nighttime ionosphere for no approximations, for the anisotropic conductor approximation [neglecting the dJ/dt term in (1)] and for the vertical $\boldsymbol{B}_E$ approximation. The nonlinear frequency scale emphasizes the characteristics of the different frequency regimes. Though not shown, neglecting the earth's magnetic field entirely is a very poor approximation for a nighttime ionosphere, as is expected because $\omega_B > \nu$ in the primary reflection region between 80–90 km altitude. We also find that the difference between a perfectly conducting ground and our assumed ground is negligible, although this difference may be significant on longer propagation paths.

The calculations in Fig. 5 show that treating the ionosphere as an anisotropic conductor is a good approximation for frequencies above ~1.5 kHz. Some of the higher frequency modal interference effects are diminished above 10 kHz, but otherwise, the agreement is very good. However, at ELF, the quasi-TEM mode is missing its fine features that are apparent in the calculation with no approximations. This weak resonance at ~300 Hz is due to wave penetration into the electron density valley centered at 140 km (see Fig. 2) and secondary reflection from the top of the valley. With the anisotropic conductor approximation, the wave damping is overestimated in this low collision frequency region and the resonance is eliminated. If modeling this feature is important for a given application, then this approximation is not appropriate. That the anisotropic conductor approximation is better at VLF than ELF is a somewhat unexpected result, as this approximation improves at a fixed altitude as frequency decreases. However, as the frequency decreases, the fields can actually penetrate to higher altitudes due to the decreasing attenuation rate where the collision frequency is lower and the approximation breaks down [43].

In contrast, the calculations show that the vertical $\boldsymbol{B}_E$ approximation is good at ELF, as the resonance is captured correctly. However, the VLF signal characteristics above 1.5 kHz are drastically changed and the quantitative agreement with the no ap-

proximations spectrum is poor. This approximation is thus valid for ELF propagation but not VLF propagation, emphasizing the importance of the horizontal $\boldsymbol{B}_E$ components in this higher frequency range.

As for the analytical approximations and FDTD, Fig. 6 shows ELF-VLF spectra computed with numerical mode theory, FDTD, and the frequency-limited Greifinger and Greifinger [37] and Sukhorukov [40] approximations. For all of these calculations we have assumed the anisotropic conductor and vertical $\boldsymbol{B}_E$ approximations, as these are implicit in the analytical approximations. No effort has been made to verify convergence of the FDTD calculations, so the disagreement with mode theory above 10 kHz is likely due to $\Delta z = 1$ km being too large for these frequencies. Nevertheless, the agreement between numerical mode theory and FDTD is extremely good below 10 kHz, validating these two techniques.

The Sukhorukov [40] analytical approximation for near-cutoff low-order modes differs from numerical mode theory by about 50%, which is quite good considering the complexity of the derivation. The quality of the Greifinger and Greifinger [37] analytical approximation varies somewhat with frequency. Below ~200 Hz, the field amplitude error is less than 10%, making this technique useful even for precise calculations in this frequency range. At higher frequencies, the error is larger but remains less than 50% up to 1 kHz. While they can be quite accurate, these analytical approximations also provide an extremely valuable understanding of the physical parameters that most strongly influence the propagation that the purely numerical solutions lack.

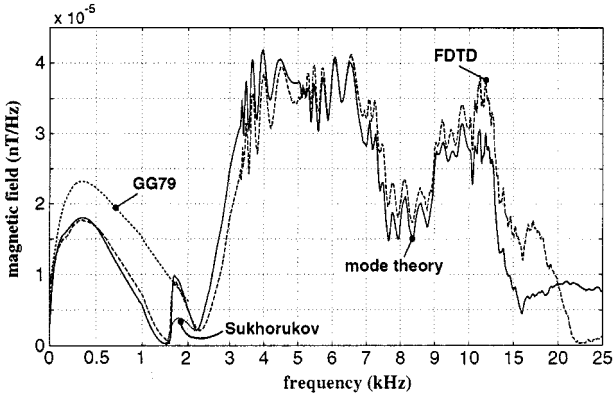

Fig. 6. Nighttime ELF-VLF spectra computed with mode theory, FDTD, and analytical approximations using the anisotropic conductor and vertical $\boldsymbol{B}_E$ ionospheric approximations. Note the nonlinearity of the horizontal scale.

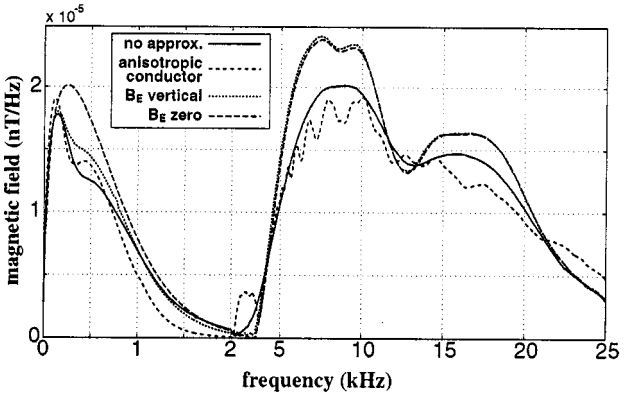

Fig. 7. Daytime ELF-VLF spectra computed with mode theory for different ionospheric approximations. Note the nonlinearity of the horizontal scale.

B. Daytime Ionosphere

The effects of the various approximations are fundamentally different for a daytime ionosphere. Fig. 7 shows horizontal magnetic field amplitude spectra for the daytime ionosphere of Fig. 2 computed with mode theory and employing the same approximations as in the previous section. Unlike the nighttime case, the anisotropic conductor approximation drastically changes the character of the VLF spectrum by increasing the amplitude of the near-cutoff modes, which is evident from the strong modal interference oscillations near the cutoff frequencies. This approximation only slightly changes the ELF portion of the spectrum, which we expect because of the absence of the electron density valley in the daytime ionosphere. In contrast to the nighttime case, we conclude that the anisotropic conductor approximation ($\nu \gg \omega$) is better at ELF than VLF for a daytime ionosphere.

As for the nighttime case, the daytime vertical $\boldsymbol{B}_E$ approximation simulation differs significantly from that with no approximations at VLF. Interestingly, if $\boldsymbol{B}_E$ is ignored entirely, then the VLF spectrum is almost identical to the vertical $\boldsymbol{B}_E$ spectrum. This highlights the importance of the horizontal components of $\boldsymbol{B}_E$ for daytime VLF propagation. At ELF, however, the vertical $\boldsymbol{B}_E$ approximation causes only small changes for daytime (as well as nighttime) propagation. The ELF spectrum changes significantly as a result of completely ignoring $\boldsymbol{B}_E$, highlighting the importance of the vertical components of $\boldsymbol{B}_E$ for both daytime ELF propagation. However, all of these approximations are very good for $f < 100$ Hz, suggesting that at these low frequencies, the fields are limited to altitudes sufficiently low that the condition $\nu \gg \omega, \omega_B$ is met.

Calculations with other techniques are shown in Fig. 8, which contains ELF-VLF spectra computed with numerical mode theory, FDTD, and the ELF Greifinger and Greifinger analytical approximation [37]. Once again, FDTD and mode theory agree well below 10 kHz, and we expect that if Δz were reduced below 1 km in the FDTD solution, the two techniques would agree better at higher frequencies. The daytime analytical approximation is very good below 1 kHz and nearly perfect below 100 Hz. We expect this analytical approximation to be more accurate for daytime than nighttime propagation because the daytime ionosphere is more closely approximated by the exponentially increasing conductivity assumed in the derivation.

C. Computational Efficiency of Mode Theory and FDTD

Since the mode theory and FDTD solutions are in close agreement, the computational efficiency of the two methods was compared on a 300 MHz Sun Ultra 2 workstation. The FDTD solution used a 1010 by 100 grid (excluding the PML layers) with 14 coefficients and field values (including values from the previous time step required by the calculations) per non-PML grid point. The memory requirement for the PML cells almost equaled that

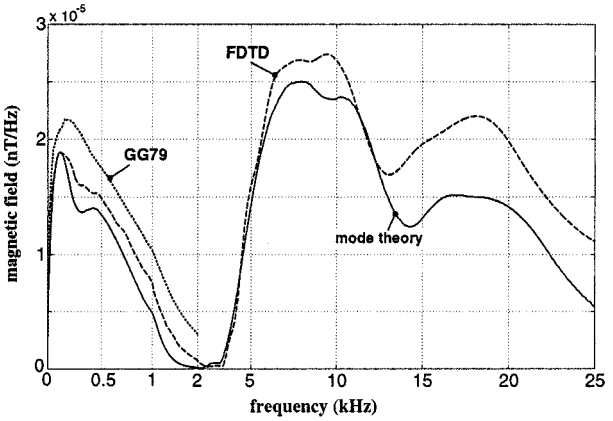

Fig. 8. Daytime ELF-VLF spectra computed with mode theory, FDTD, and analytical approximations using the anisotropic conductor and vertical $\boldsymbol{B}_E$ ionospheric approximations. Note the nonlinearity of the horizontal scale.

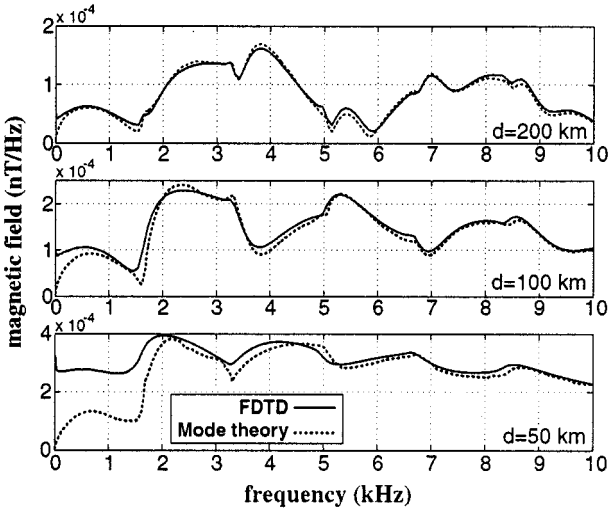

Fig. 9. Nighttime ELF-VLF spectra computed with mode theory and FDTD for $d = 50$, 100, and 200 km from the source.

for the non-PML cells because of the large number of PML variables and coefficients required in cylindrical coordinates and the relatively deep (40 and 80 cells) PML layers required to attenuate the low frequency fields. In entirety, this FDTD simulation used about 28 Mb of memory, with all variables stored as 8-b words. The total processing time required for 5000 time steps (12 ms of simulated fields) was 84 min, giving a sustained floating point operation rate of 11.8 Mflops. No effort was made to reduce the number of floating point operations in the simulation, so the processing time could possibly be reduced by 10–20% by renormalizing certain variables.

In contrast, the mode theory simulations only required a few megabytes of memory, as the only numerical integrations in the code are one-dimensional (1-D). The mode theory computational effort was dominated by the eigenangle calculation. For a horizontally homogeneous propagation path, calculating the modal eigenangles from 0–25 kHz took 31 minutes. While the memory requirements are more than an order of magnitude higher for the FDTD method, the simulation times differ by only a factor of three, making FDTD very competitive on modern computers.

Interestingly, the two techniques scale very differently with problem size and characteristics. If the propagation path is contains horizontal inhomogeneities, then the mode theory computation must be segmented and the eigenangles must be found separately for each segment [30]. Thus, the mode theory simulation time scales linearly with the number of sharp horizontal inhomogeneities. However, the mode theory simulation time is independent of propagation distance because the complexity of the mode sum in (5) does not vary with distance. The FDTD simulation time, of course, scales linearly with propagation distance (for a fixed spatial step size), while additional inhomogeneities do not affect the FDTD simulation time.

D. Source Proximity and Post-Discharge Currents

One of the primary strengths of mode theory at long distances from the source is its compact representation of the fields in terms of just a few dominant modes. This strength becomes a weakness at distances close to the source, where even evanescent modes can contribute significantly to the fields. To investigate the validity of mode theory over short propagation paths, we compare FDTD and mode theory solutions at $d = 50$, 100, and 200 km from the source. Fig. 9 shows these results. At $d = 200$ km, mode theory and FDTD agree well for all frequencies except lower ELF. Even as close as $d = 50$ km, mode theory is quite accurate above 5 kHz, verifying the rule of thumb that evanescent modes are not significant when the propagation distance is greater than a wavelength. Some of the disagreement near 1.6 and 3.2 kHz for $d = 50$ and 100 km is due to the evanescent quasi-TE_1 and quasi-TM_1 modes contributing to the signal, as was shown analytically in [33].

However, the calculations also disagree at the bottom of the ELF range. At $d = 200$ km, the FDTD signal falls off more slowly with frequency below 500 Hz. At $d = 100$ km the disagreement extends up to 1 kHz and at $d = 50$ km to 2 kHz. And at all three distances, the FDTD spectral amplitudes increase sharply below a few tens of hertz. These fields are produced by the abovementioned post-discharge ionospheric relaxation currents, which mode theory does not directly include but FDTD does. Charge is deposited in the cloud as a result of the lightning discharge as a result of the zero frequency excitation in the source. Along with the image charge in the ground, this charge creates a dipolar electrostatic field (a plot of $|\boldsymbol{E}|$ would show this electrostatic field with a dipolar r^{-3} decay). This electrostatic field attracts charge from the conducting ionosphere and creates a downward moving layer of charge that represents the boundary between conduction and displacement current [35]. The downward velocity of this layer depends on the local dielectric relaxation time of the ionosphere. The presence of this moving charge layer means that conduction currents must exist in the ionosphere in order to move the charge. These currents create their own post-discharge electric and magnetic fields, which were derived analytically by Greifinger and Greifinger in an elegant paper [35]. This solution is hereafter referred to as the GG solution

Fig. 10 shows that these post-discharge ionospheric relaxation currents bridge the gap between the mode theory and FDTD solutions. Plotted are the ELF magnetic field spectra at

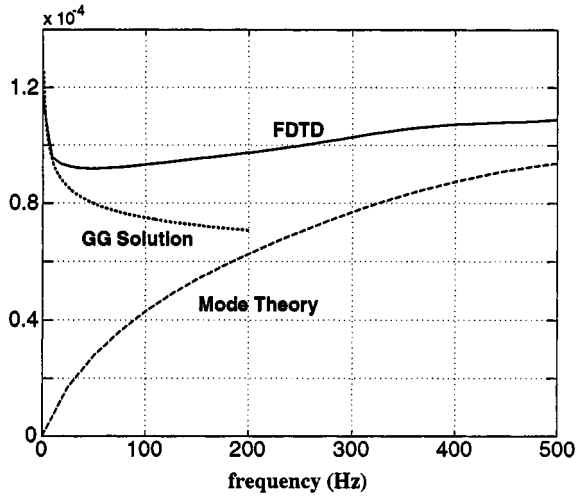

Fig. 10. Nighttime ELF spectra computed with mode theory, FDTD, and the analytical GG solution for $d = 100$ km. The post-discharge ionospheric relaxation fields of the GG solution explain the discrepancy between mode theory and FDTD.

$d = 100$ km for mode theory, FDTD, and the GG solution. For $f < 20$ Hz, the FDTD and GG solutions are essentially identical, while above this frequency the FDTD solution is roughly the expected combination of mode theory and the GG solution. As shown in Fig. 9, for $f > 1$ kHz, the FDTD and mode theory fields converge and the ionospheric relaxation fields are negligible. A careful combination of the GG solution and mode theory can thus describe the complete EM fields produced by a lightning discharge which are automatically calculated with the FDTD technique, as in the approximate analytical formulation in [33]. The frequencies for which these post-discharge fields are significant depend strongly on the distance from the source. FDTD and mode theory solutions show that at 700 km, the ionospheric relaxation fields are only significant below ~ 50 Hz, while at 100 km, Fig. 9 shows that the relaxation fields are significant up to $\sim$500 Hz. This demonstrates that care must be taken in interpreting short distance ELF field observations distances with mode theory alone.

VI. Conclusion

With a series of mode theory, FDTD, and approximate analytical simulations of propagation from lightning-generated ELF-VLF radiation in the earth–ionosphere waveguide, we have examined the accuracy of each of these techniques. We have demonstrated that mode theory can agree extremely well with ELF-VLF observations when the ionosphere is treated as a inhomogeneous anisotropic cold plasma, thereby validating the technique that we use as the benchmark solution. At ELF, the mode theory solutions show that the horizontal components of $\boldsymbol{B}_E$ can be neglected for both daytime and nighttime ionospheres without much effect. At VLF, however, the horizontal and vertical $\boldsymbol{B}_E$ components have a major effect on the solution. The ionosphere can accurately be treated as an anisotropic conductor ($\nu \gg \omega$) for nighttime VLF propagation, but for daytime VLF propagation this approximation strongly decreases the attenuation for near-cutoff waveguide modes. And, surprisingly, the anisotropic conductor approximation for nighttime ELF propagation eliminates some significant propagation characteristics observable in the solution with no approximations. The ELF and near-cutoff approximate analytical solutions are found to be reasonably accurate (10–50%) in comparison to the numerical mode theory calculations. And mode theory and FDTD agree very well over most of the ELF-VLF frequency range. The high frequency disagreement ($>$10 kHz) is attributed to insufficient spatial (we chose $\Delta z = 1$ km) and temporal resolution in the FDTD solution.

By comparing FDTD and mode theory solutions, we also find that mode theory gives generally good results at VLF at distances as short as 100 km from the source. However, for frequencies less than $\sim$2 kHz, the difference between mode theory and FDTD grows as frequency and distance decrease. We attribute this difference to two factors. First, evanescent modes excited by the lightning discharge contribute to the fields when the propagation distance is short. With care in calculating the characteristics of the evanescent modes, however, mode theory can account for these fields. Second, the zero frequency component of the lightning source (i.e., the net charge motion) combined with the increasing ionospheric conductivity with altitude create long-lasting post-discharge currents in the ionosphere which generate their own EM fields. These post-discharge fields are not accounted for in traditional mode theory but are implicitly generated in the FDTD solution. We find that the gap between the mode theory and FDTD solutions is largely accounted for by an approximate analytical solution for the post-discharge fields [35]. These post-discharge fields can be significant for $f \lesssim 500$ Hz over short propagation paths and may need to be accounted for in interpreting ELF lightning observations. A major strength of the FDTD technique for this problem is that all the fields (discharge and post-discharge, evanescent and propagating) are automatically calculated, while most other solution techniques are forced to treat these fields separately. While mode theory calculations over long propagation distances can be very efficient and faster than FDTD, the simplicity of FDTD propagation modeling and ever-increasing computer power probably make FDTD the technique of the future. However, the physical insight provided by Wait's and others' mode theory is indispensable for understanding the propagation problem and interpreting purely numerical simulations.

References

[1] E. D. Kaplan, Ed., *Understanding GPS: Principles and Applications*. Norwood, MA: Artech House, 1996.
[2] R. A. Dana, "Effects of ionospheric scintillation on differential demodulation of GPS data," *IEEE Trans. Aerosp. Electron. Syst.*, vol. 33, p. 893, July 1997.
[3] K. Davies, *Ionospheric Radio*. Stevenage, U.K.: Peter Peregrinus, 1990.
[4] A. L. Green, "Early history of the ionosphere," *J. Atmos. Terrestrial Phys.*, vol. 36, p. 2159, 1974.
[5] J. R. Wait, "Terrestrial propagation of very-low-frequency radio waves, a theoretical investigation," *J. Res. Nat. Bureau Stand.*, vol. 64D, p. 153, 1960.
[6] J. R. Wait and K. P. Spies, "Influence of finite ground conductivity on the propagation of VLF radio waves," *J. Res. Nat. Bureau Stand.*, vol. 69D, p. 1359, 1965.
[7] J. R. Wait, "On phase changes in very-low-frequency propagation induced by an ionospheric depression of finite extent," *J. Geophys. Res.*, vol. 69, p. 441, 1964.

[8] ——, "Reflection of VLF radio-waves at a junction in the earth ionosphere waveguide," *IEEE Trans. Electromagn. Compat.*, vol. 34, p. 4, Feb. 1992.
[9] ——, "EM scattering from a vertical column of ionization in the earth-ionosphere waveguide," *IEEE Trans. Antennas Propagat.*, vol. 39, p. 1051, 1991.
[10] S. A. Cummer, U. S. Inan, and T. F. Bell, "Ionospheric D region remote sensing using VLF radio atmospherics," *Radio Sci.*, vol. 33, p. 1781, 1998.
[11] U. S. Inan, A. Slingeland, V. P. Pasko, and J. V. Rodriguez, "VLF and LF signatures of mesospheric lower ionospheric response to lightning discharges," *J. Geophys. Res.*, vol. 101, p. 5219, 1996.
[12] C. J. Rodger, N. R. Thomson, and J. R. Wait, "VLF scattering from red sprites: vertical columns of ionization in the earth-ionosphere waveguide," *Radio Sci.*, vol. 34, p. 913, 1999.
[13] U. S. Inan, S. C. Reising, G. J. Fishman, and J. M. Horack, "On the association of terrestrial gamma-ray bursts with lightning and implications for sprites," *Geophys. Res. Lett.*, vol. 23, p. 1017, 1996.
[14] S. A. Cummer and U. S. Inan, "Modeling ELF radio atmospheric propagation and extracting lightning currents from ELF observations," Radio Sci., 1999, to be published.
[15] E. Huang, E. Williams, R. Boldi, S. Heckman, W. Lyons, M. Taylor, T. Nelson, and C. Wong, "Criteria for sprites and elves based on Schumann resonance observations," *J. Geophys. Res.*, vol. 104, p. 16943, 1999.
[16] S. A. Cummer, U. S. Inan, T. F. Bell, and C. P. Barrington-Leigh, "ELF radiation produced by electrical currents in sprites," *Geophys. Res. Lett.*, vol. 25, p. 1281, 1998.
[17] W. A. Lyons, "Sprite observations above the U.S. high plains in relation to their parent thunderstorm systems," *J. Geophys. Res.*, vol. 101, p. 29 641, 1996.
[18] E. R. Williams, "The Schumann resonance—A global tropical thermometer," *Sci.*, vol. 256, p. 1184, 1992.
[19] D. W. Strangway, C. M. Swift, and R. C. Holmer, "The application of audio-frequency magnetotellurics (AMT) to mineral exploration," *Geophys.*, vol. 38, p. 1159, 1975.
[20] O. A. Molchanov and M. Hayakawa, "Subionospheric VLF signal perturbations possibly related to earthquakes," *J. Geophys. Res.*, vol. 103, p. 17 489, 1998.
[21] M. Parrot, "Statistical study of ELF/VLF emissions recorded by a low-altitude satellite during seismic events," *J. Geophys. Res.*, vol. 99, p. 23 339, 1994.
[22] K. G. Budden, *The Wave-Guide Mode Theory of Wave Propagation*. London, U.K.: Logos, 1961.
[23] K. Baba and M. Hayakawa, "The effect of localized ionospheric perturbations on subionospheric VLF propagation on the basis of finite-element method," *Radio Sci.*, vol. 30, p. 1511, 1995.
[24] J. R. Wait, *Electromagnetic Waves in Stratified Media*. Oxford, U.K.: Pergamon, 1970.
[25] J. Galejs, *Terrestrial Propagation of Long Electromagnetic Waves*. Oxford, U.K.: Pergamon, 1972.
[26] Y. N. Taranenko, U. S. Inan, and T. F. Bell, "Interaction with the lower ionosphere of electromagnetic pulses from lightning—Heating, attachment, and ionization," *Geophys. Res. Lett.*, vol. 20, p. 1539, 1993.
[27] K. G. Budden, *The Propagation of Radio Waves*. Cambridge, U.K.: Cambridge Univ. Press, 1985.
[28] J. K. Hargreaves, *The Solar-Terrestrial Environment*. Cambridge, U.K.: Cambridge Univ. Press, 1992.
[29] K. G. Budden, "The influence of the earth's magnetic field on radio propagation by wave-guide modes," *Proc. Roy. Soc. A*, vol. 265, p. 538, 1962.
[30] R. A. Pappert and J. A. Ferguson, "VLF/LF mode conversion model calculations for air to air transmissions in the earth-ionosphere waveguide," *Radio Sci.*, vol. 21, p. 551, 1986.
[31] J. A. Stratton, *Electromagnetic Theory*. New York: McGraw-Hill, 1941.
[32] J. Kraus, *Electromagnetics*. New York: McGraw-Hill, 1992.
[33] A. I. Sukhorukov, "Lightning transient fields in the atmosphere-low ionosphere," *J. Atmos. Terrestrial Phys.*, vol. 58, p. 1711, 1996.
[34] D. L. Jones, "Electromagnetic radiation from multiple return strokes of lightning," *J. Atmos. Terrestrial Phys.*, vol. 32, p. 1077, 1970.
[35] C. Greifinger and P. Greifinger, "Transient ULF electric and magnetic fields following a lightning discharge," *J. Geophys. Res.*, vol. 81, p. 2237, 1976.
[36] M. E. Baginski, L. C. Hale, and J. J. Olivero, "Lightning-related fields in the ionosphere," *Geophys. Res. Lett.*, vol. 15, p. 764, 1988.
[37] C. Greifinger and P. Greifinger, "Ionospheric parameters which govern high latitude ELF propagation in the Earth-ionosphere waveguide," *Radio Sci.*, vol. 14, p. 889, 1979.
[38] ——, "Approximate method for determining ELF eigenvalues in the Earth-ionosphere waveguide," *Radio Sci.*, vol. 13, p. 831, 1978.
[39] J. R. Wait, "On ELF transmission in the earth ionosphere waveguide," *J. Atmos. Terrestrial Phys.*, vol. 54, p. 109, 1992.
[40] A. I. Sukhorukov, "ELF-VLF atmospheric waveforms under night-time ionospheric conditions," *Ann. Geophys.*, vol. 14, p. 33, 1993.
[41] M. Hayakawa, K. Ohta, and K. Baba, "Wave characteristics of tweek atmospherics deduced from the direction-finding measurement and theoretical interpretation," *J. Geophys. Res.*, vol. 99, p. 10 733, 1994.
[42] F. L. Teixeira and W. C. Chew, "PML-FDTD in cylindrical and spherical grids," *IEEE Microwave Guided Wave Lett.*, vol. 7, p. 285, Sept. 1997.
[43] S. A. Cummer and U. S. Inan, "Ionospheric E region remote sensing with ELF radio atmospherics," Radio Sci., 2000, to be published.

Steven A. Cummer (S'91–M'97) received the B.S. (with distinction), M.S., and Ph.D. degrees in electrical engineering from Stanford University, Stanford, CA, in 1991, 1993, and 1997, respectively.

From 1997 to 1999, he was a National Research Council Postdoctoral Research Associate at NASA Goddard Space Flight Center, Greenbelt, MD. He is currently an Assistant Professor in the Electrical and Computer Engineering Department, Duke University. His current research activities include electromagnetic propagation modeling in complex media, ionospheric remote sensing, lighting, and inverse methods.

Dr. Cummer received the Outstanding Student Paper Award at the 1994 American Geophysical Union Fall Meeting and was a finalist in the Student Paper competition at the 1995 IEEE Antennas and Propagation Society International Symposium. He received the International Union of Radio Science (URSI) Young Scientist Award in 1999. He is a Member of the URSI Commission H, the American Geohysical Union, and Sigma Xi.